Automatic Feature Extraction of Optical Coherence Tomography for Lamina Cribrosa Detection

Mei Hui Tan
NUS Graduate School for Integrative Sciences and Engineering, National University of Singapore, Singapore
Email: mei.hui@u.nus.edu

Sim Heng Ong
Department of Electrical and Computer Engineering, National University of Singapore, Singapore
Email: eleongsh@nus.edu.sg

Sri Gowtham Thakku, Ching-Yu Cheng, and Tin Aung
Singapore Eye Research Institute, Singapore National Eye Centre, Singapore
Email: gowtham@invivobiomechanics.com, ching-yu_cheng@nuhs.edu.sg, aung.tin@snec.com.sg

Michael Girard
Department of Biomedical Engineering, National University of Singapore, Singapore
Email: mgirard@nus.edu.sg

***Abstract*—This paper presents a framework to segment and extract key features automatically in Optical Coherence Tomography (OCT) scans. One of the main features to be detected is the Lamina Cribrosa (LC), which is an optic nerve head structure believed to play a crucial role in glaucomatous optic neuropathy. Detection of the LC aids in understanding pathogenesis and detection of glaucoma. Automatic segmentation allows a quick and objective way of identifying the LC. In previous work, LC segmentation has been manual; hence, the aim is to achieve automatic and accurate segmentation. Automatic detection is a novel approach, and very important as it provides an objective and fast way to identify the features. The method consists of three steps: automatic detection of the Bruch's membrane opening, definition of LC Region of Interest (ROI), and feature detection in the ROI using local and inter-frame information. The best-fit curve representing the anterior LC was obtained by optimizing parameters to minimize the inter-frame gradient and local gradient change. The algorithm was applied to OCT images captured by Spectralis OCT machine (Heidelberg Engineering GmbH, Heidelberg, Germany). The results were compared and verified against manual segmentation of the key features, with a Root-Mean-Square (RMS) error of 9.89 and Dice coefficient of 0.74. The generally accurate results indicate that the approach is highly promising, and could potentially be expanded across detection in other image types.**

***Index Terms*—automatic segmentation, Bruch's membrane, feature detection, lamina cribrosa, optical coherence tomography**

I. Introduction

Glaucoma is an eye disease in which high fluid pressure within the eye damages delicate fibers of the optic nerve. It is the leading cause of irreversible blindness worldwide. The global prevalence of glaucoma among those above 40 years old is 2.65% [1].

The LC is a thin, sieve-like portion of the sclera at the base of the optic disc through which retinal nerve fibers leave the eye to form the optic nerve (Fig. 1). It helps to maintain the gradient between the inside of the eye and the surrounding tissues. It bulges slightly outwards due to intra-ocular pressure. It has been shown that defects and changes in the LC are possible indicators of glaucoma progression [2], as the LC may be displaced. The idea was first proposed in 1981 [3]. The visual field loss occurs due to optic nerve damage. The pattern and degree of visual field loss has a correlation with glaucoma. Other studies also indicate that the biomechanics in the sclera and strain in the LC play a role in glaucoma progression [4]. We propose a framework to perform automatic feature detection using OCT, in particular the segmentation of the anterior LC. In previous studies of the LC, the identification was done using manual methods [5], [6]. Our method allows for automatic segmentation based on landmarks present in the image in our method. One of the main challenges is the general lack of details available in OCT images. The visualization of LC is often difficult due to artifacts, shadows and low contrast of the images. We perform shadow removal and contrast enhancement to improve the image quality as a pre-processing step [7].

Manuscript received January 14, 2015; revised August 26, 2015.

doi: 10.18178/joig.3.2.102-106

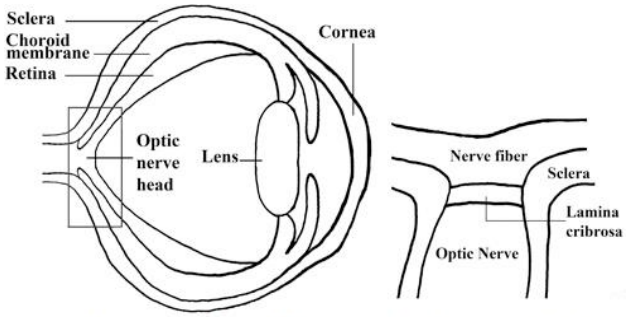

(a) Horizontal section of the eye (b) Location of lamina cribrosa

Figure 1. Location of lamina cribrosa in the optic nerve.

II. Proposed Framework

The proposed framework consists of three main steps (Fig. 2): (1) automatic detection of Bruch's membrane opening; (2) ROI identification and (3) lamina cribrosa detection.

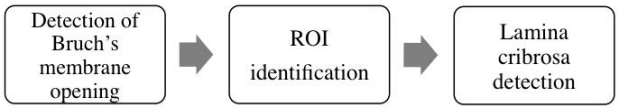

Figure 2. Proposed framework.

A. Automatic Detection of Bruch's Membrane Opening

The LC lies below the Bruch's membrane opening. The Bruch's membrane is the innermost layer of the choroid, and comprises of five layers [8]. In the OCT image, the layers of the Bruch's membrane can be identified from their gray levels. Among the five layers, one particular layer appears distinctly as a brighter line. The line is disjointed around the location of the Bruch's membrane opening for slices in the OCT where the membrane opening is visible. This is an important and distinct landmark to determine the location of the Bruch's membrane.

For each layer in the Bruch's membrane, the gray level and texture is generally homogeneous. Hence, the vertical mean gray level for each column across the Bruch's membrane would yield a similar value. The region within the Bruch's membrane opening has a significant change in texture and gray level, so the mean gray level computed vertically would provide a very different value.

First, the dark and uniform region above the Bruch's membrane is discarded from the original image. This can be done automatically by obtaining the average gray level across rows of the image, and excluding rows with low gray level mean. Subsequently, m_i, the mean gray level of each column i is calculated. The change in consecutive mean column value, $\Delta m_i = |m_{i+1} - m_i|$ is tabulated. Δm_i measures the gradient of the mean. The greatest change in Δm_i is detected from two directions– one from the left and one from the right. In Fig. 3(a), the first major peaks from the left and right of the plot represent the Bruch's membrane opening point. The selected peaks are marked by 'x'. The corresponding columns are highlighted in Fig. 3(b).

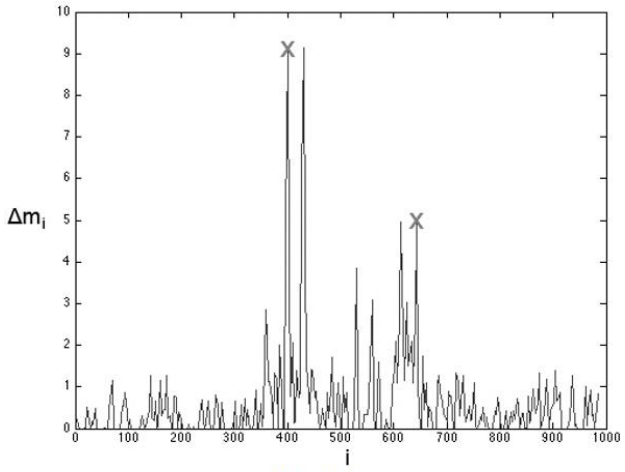

(a) Plot of Δm_i

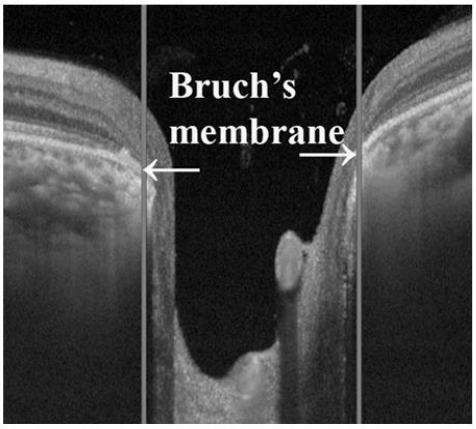

(b) Columns identifying the Bruch's membrane opening

Figure 3. Identifying Bruch's membrane using Δmi, selected peaks marked in crosses.

B. ROI Identification

The region bounded between the two columns representing Bruch's membrane opening is then extracted. There are 3 major anatomical structures present in the ROI- the nerve fiber, LC and optic nerve. This process is a fast and accurate way to estimate the general region where the anterior LC can be detected.

The first step is to separate the regions outside the nerve fiber, and the combined areas comprising the nerve fiber, LC and optic nerve. Noise and general artifacts were first removed by smoothing and down-sampling. K-means clustering was then applied to the ROI with $k = 4$ to give four main clusters. The value was selected experimentally by comparing the clusters to manual labels. The four clusters can be approximated to represent the background, nerve fiber, LC and optic nerve. Basic morphological operations were applied to remove small clusters and noise, ensuring smoothness and continuity. The result obtained using k-means is sufficient to differentiate the layers and each cluster is shown to represent a good estimate of the anatomy.

C. Lamina Cribrosa Detection

An estimate of where the LC can now be determined. A seed curve is based on the demarcation between the top 2 cluster layers. The local gradient for points across the seed curve was computed. The gradient, g, is computed by:

$$g = \frac{\left| a_{R_1} - a_{R_2} \right|}{S_{R_1} + R_2} \quad (1)$$

R_1 and R_2 are regions above and below the tangent line with respect to the point on the curve (Fig. 4). The radius of the mask for R_1 and R_2 is fixed at 10 pixels to ensure that the gradient is localized. The gradient is computed for points with horizontal intervals of 15 pixels in (1). S_{R1+R2} refers to the total number of pixels in regions R_1 and R_2, and a is the average gray value in the region. If the value of g is close to 0, the point is discarded as it may indicate that the region is homogeneous and does not provide much information on the LC. Lack of gradient change will occur at regions of low contrast or shadows.

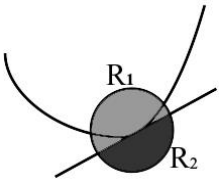

Figure 4. Determining R_1 and R_2.

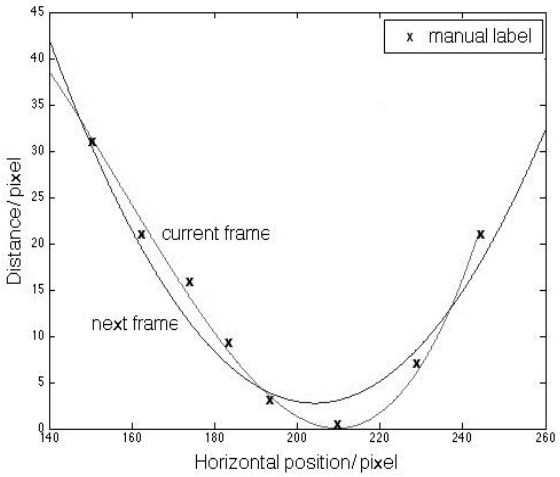

Figure 5. Comparison of manual labels and segmentation results between frames.

Based on the new points obtained, a best-fit curve is plotted. The curve is optimized by

$$\alpha = \sum_x w_1 \Delta d_x + w_2 \Delta c_x + w_3 \Delta f_x \quad (2)$$

The neighborhood to be searched is within 15 pixels from the reference point. α will be minimized for the set of all detected points x. Δd_x is the change in distance from the current point to the updated point. Δd_x ensures that the proximity of the updated point is not too far from the previous point.

$$\Delta c = \left| g_t - g_{t+1} \right| \quad (3)$$

It is the change in gradient between the current point and the updated point. t in (3) refers to the iteration number.

$$\Delta f = \left| g_i - g_{i+1} \right| \quad (4)$$

It is the change in gradient between the current point in the reference frame and the current point in the next frame. i in (4) refers to the frame reference where $i + 1$ is the next frame. The value of w_1 and w_2 are set as 0.45, while w_3 is set at 0.1. The inter-frame comparison in (4) is given a lower weight as the orientation and scaling factors between frames may sometimes cause the value of f to be higher. This can be seen in Fig. 5 where the best-fit curve of the current frame and next frame are slightly different.

III. Experimetns and Results

The data used was from the Singapore Eye Research Institute (SERI). ONH raster scans were performed on the right and left eyes of 20 subjects on the Spectralis OCT machine (Heidelberg Engineering GmbH, Heidelberg, Germany). The Enhanced Depth Imaging (EDI) feature was chosen to improve image contrast and visualization of deep ONH structures [9], [10]. 2 scans were performed per eye for 2 visits. Each set of images comprised 72 serial horizontal sectional scans covering a rectangular region of 15×15 degrees centered on the optic nerve head. To reduce speckle noise, each sectional scan was also averaged from 20 captured frames. Not every frame contains details of the LC and Bruch's membrane opening; hence for each scan session, only 2 consecutive frames were selected for segmentation. The data were manually labeled by 2 experienced clinicians, with the Bruch's membrane opening and points along the anterior LC identified. These labels were taken as the ground truth for comparison.

In addition, shadow removal and image contrast improvement was performed on the Spectralis data set using *Reflectivity 3.2* [11]. Often, the OCT images have parts of the ROI occluded due to shadows from blood vessels. Reflectivity successfully removes most of these shadows. The parameters used for shadow removal and compensation were fixed at default values for all images processed to ensure image comparability.

Based on the data used, the mean distance of points on the final fitted curve obtained from the ground truth was 8.52 pixels. The Root-Mean-Square (RMS) error for all points considered was 9.89 pixels. An example of a good detection result is shown in Fig. 6(a). The RMS error and mean distance is within acceptable range for an accurate detection of the major landmarks required to trace the anterior LC. The black points represent the points detected automatically, while the white points indicate manual labels.

The result was further broken down to consider the ROI as three sections (Fig. 6(c)). The ROI was divided into three equal columns for each image, representing the left (L), center (C) and right (R) regions. The average distance of the detected point from the ground truth for each region was computed. For the left region, the mean

distance was 8.32, center region was 13.18 pixels and right region was 5.62 pixels. The results can be attributed to the presence of shadows mainly occurring close to the center region, hence there was more ambiguity in the detected points due to poor contrast and shadows present. In addition, some of the discrepancies were due to the detection of the change in gradient close to the edge of a vertical shadow (Fig. 6(b)). For image samples that do not have major artifacts or shadows present, the results were close to the ground truth.

The Dice coefficient was also computed. The region considered was based on the areas within 10 pixels from the manual best-fit curve and the anterior LC boundary obtained through automated segmentation. The overlap in the regions can be visualized on the OCT (Fig. 6(d)). The overall Dice coefficient within the ROI was 0.74. Furthermore, the Dice coefficients of the left, center and right regions of the ROI were determined to be 0.73, 0.68 and 0.75 respectively. The Dice coefficient provides an indicator of the segmentation results, and as with the RMS error the agreement was lower in the center region than the left and right regions.

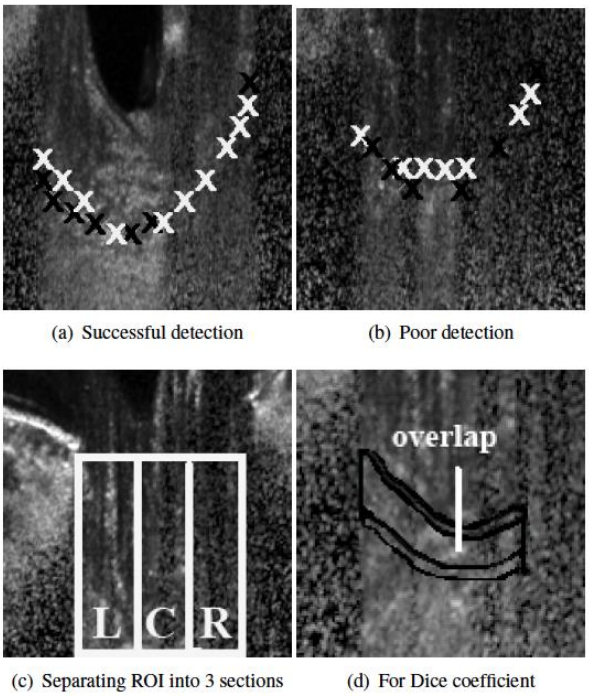

(a) Successful detection (b) Poor detection

(c) Separating ROI into 3 sections (d) For Dice coefficient

Figure 6. Results of automatic segmentation.

IV. Discussion and Conclusion

We have introduced a new framework that automatically segments features in OCT optic nerve head images, in particular the anterior LC. The identification of the features was based on the location of the Bruch's membrane opening. The determination of the ROI and anterior LC detection was automatic and based on seed points identified. The optimization is performed based on minimizing the inter-frame gradient and local gradient change. With an objective method of segmentation, the results can be compared with manual segmentation. The segmentation outcome based on the RMS error and Dice coefficient is promising, with RMS error of 9.89 and Dice coefficient of 0.74. It is shown that the curve obtained is in close agreement with the manual curve.

We hope to extend the framework to account for scaling between frames, and include more data from different clinical studies to compare the results.

Acknowledgment

We wish to thank Dr. Mani Baskaran of Singapore Eye Research Institute, Singapore for his work on the medical data. The authors would also like to thank Dr. Jean Martial Mari from University of French Polynesia, France and Dr. Nicholas Strouthidis from Moorfields Eye Hospital, London for the use of *Reflectivity 3.2*.

References

[1] H. A. Quigley and A. T. Broman, "The number of people with glaucoma worldwide in 2010 and 2020," *British Journal of Ophthalmology*, vol. 90, no. 3, pp. 262-267, 2006.

[2] S. Kiumehr, S. C. Park, D. Syril, C. C. Teng, C. Tello, J. M. Liebmann, and R. Ritch, "In vivo evaluation of focal lamina cribrosa defects in glaucoma," *Archives of Ophthalmology*, vol. 130, no. 5, pp. 552-559, 2012.

[3] H. A. Quigley and E. M. Addicks, "Regional differences in the structure of the lamina cribrosa and their relation to glaucomatous optic nerve damage," *Archives of Ophthalmology*, vol. 99, no. 1, pp. 137-143, 1981.

[4] R. E. Norman, J. G. Flanagan, I. A. Sigal, S. M. Rausch, I. Tertinegg, and C. R. Ethier, "Finite element modeling of the human sclera: influence on optic nerve head biomechanics and connections with glaucoma," *Experimental Eye Research*, vol. 93, no. 1, pp. 4-12, 2011.

[5] A. S. Vilupuru, N. V. Rangaswamy, L. J. Frishman, E. L. S. Lii, R. S. Harwerth, and A. Roorda, "Adaptive optics scanning laser ophthalmoscopy for in vivo imaging of lamina cribrosa," *JOSAA*, vol. 24, no. 5, pp. 1417-1425, 2007.

[6] A. Bhandari, A. Fontana, F. W. Fitzke, and R. A. Hitchings, "Quantitative analysis of the lamina cribrosa in vivo using a scanning laser opthalmoscope," *Current Eye Research*, vol. 16, no. 1, pp. 1-8, 2007.

[7] M. Girard, N. G. Strouthidis, C. R. Ethier, and J. M. Mari, "Shadow removal and contrast enhancement in optical coherence tomography images of the human optic nerve head," *Investigative Ophthalmology & Visual Science*, vol. 52, no. 10, pp. 7738-7748, 2011.

[8] J. C. Booij, D. C. Baas, J. Beisekeeva, T. Gorgels, and A. Bergen, "The dynamic nature of Bruch's membrane," *Progress in Retinal and Eye Research*, vol. 29, no. 1, pp. 1-18, 2010.

[9] I. A. Sigal, B. Wang, N. G. Strouthidis, T. Akagi, and M. J. Girard, "Recent advances in OCT imaging of the lamina cribrosa," *British Journal of Ophthalmology*, vol. 98, no. 2, pp. ii34-ii39, 2014.

[10] R. F. Spaide, H. Koizumi, and M. C. Pozonni, "Enhanced depth imaging spectral-domain optical coherence tomography," *American Journal of Ophthalmology*, vol. 146, no. 4, pp. 496-500, 2008.

[11] J. M. Mari, N. G. Strouthidis, S. C. Park, and M. J. Girard, "Enhancement of lamina cribrosa visibility in optical coherence tomography images using adaptive compensation," *Investigative Ophthalmology & Visual Science*, vol. 54, no. 3, pp. 2238-2247, 2013.

Mei Hui Tan is a Ph.D. candidate from the National University of Singapore Graduate School for Integrative Sciences and Engineering (NGS). She obtained her Bachelor of Engineering with Honours in Electrical Engineering and Minor in Technopreneurship from National University of Singapore (NUS) in 2011. Her area of research is in medical imaging and visualization.

Sim Heng Ong is an Associate Professor with the Department of Electrical and Computer Engineering at NUS. He obtained his B.E. (Hons) from University of Western Australia and Ph.D. from The University of Sydney. His major research areas are computer vision, medical image analysis and visualization. He collaborates extensively with clinicians from the National University Hospital, Singapore, in the analysis and visualization of a variety of medical images with the aim of developing software tools that will assist medical doctors in diagnosis, treatment planning and patient monitoring.

Sri Gowtham Thakku is a Research Officer with the Singapore Eye Research Institute (SERI) and obtained his undergraduate degree in Mechanical Engineering from the National University of Singapore (NUS). He has experience in applying image processing and computational techniques to better characterize the morphology of ocular structures that play a crucial role in the progression of eye disease.

Ching-Yu Cheng is an Associate Professor at Academic Medicine Research Institute, Duke-NUS Graduate Medical School and the Head of Ocular Epidemiology Research Group and Statistics Unit at Singapore Eye Research Institute. He is also with the Department of Ophthalmology at NUS. His primary research interests are related to the epidemiology and genetics of major eye diseases. His current work involves in a variety of epidemiological, clinical, and image research on glaucoma; and identification of susceptibility genes for complex ocular diseases, such as glaucoma, age-related macular degeneration and cataract, using both genome-wide association approaches and next-generation sequencing technology.

Tin Aung is a clinician-scientist and leads the Glaucoma Research Group at Singapore National Eye Centre and Singapore Eye Research Institute (SNEC/SERI). After receiving his MBBS and Master of Medicine in Ophthalmology from the NUS, Prof Aung obtained the Fellowships of the Royal College of Surgeons of Edinburgh and the Royal College of Ophthalmologists in 1997. He completed a glaucoma fellowship in the Singapore National Eye Centre in 1999-2000, and from 2000-2003, he was trained at Moorfields Eye Hospital in London and the Institute of Ophthalmology, University College London. In 2003, Prof Aung was awarded a PhD in Molecular Genetics from University College London, UK.

Prof Aung's main research interests are angle closure glaucoma and the molecular genetics of eye diseases. Prof Aung is very active in clinical glaucoma research and has conducted many studies on therapeutics, imaging, screening, clinical course and surgical outcomes of glaucoma.

Prof Aung is currently Associate Executive Vice President of the World Glaucoma Association and a Board member of the South East Asia Glaucoma Interest Group (SEAGIG) and the Asian Angle Closure Glaucoma Club. In Singapore, he is President Elect of the College of Ophthalmologists of Singapore and immediate past President of the Singapore Society of Ophthalmology. He is also the Academic Vice Chair (Research) of the Academic Clinical Program for Ophthalmology in SingHealth/Duke-NUS Graduate School of Medicine.

Michael Girard is an Assistant Professor in the Department of Biomedical Engineering at National University of Singapore. He received his engineering diploma in Mechanical Engineering from the Ecole Polytechnique Universitaire de Lyon, France in 2003. He was awarded his PhD from the Department of Biomedical Engineering at Tulane University, New Orleans, USA, in January of 2009. Subsequently, Dr. Girard pursued his postdoctoral work in the Department of Bioengineering at Imperial College London, UK. In September of 2010, Dr. Girard was awarded a highly competitive and prestigious Imperial College Junior Research Fellowship to pursue his research. Throughout his training, Dr. Girard has gained expertise in experimental, theoretical, and computational soft tissue biomechanics, which he has utilized to pose and answer questions of high clinical relevance in the field of ophthalmology. Dr. Girard's current research program aims to develop state-of-the-art engineering tools for the diagnosis and treatment of biomechanically-related pathologies.